

# The Fracture of Rock around Underground Openings

By

Yoshio HIRAMATSU and Yukitoshi OKA\*

(Received January 31, 1959)

The authors have carried out researches on the mechanism of the failure of rocks which is found at underground openings by means of experiments with models and stress analysis by photoelasticity as well as by field observations and arrived at the following conclusion. The fracture of rock on the inner surface of underground openings takes place when the theoretical maximum stress, tensile or compressive, under the assumption that the ground is perfectly elastic, multiplied by a corresponding factor reaches the tensile or compressive strength of the rock. There is a great difference between the factors for tension and compression fracture, namely that the former is about 0.45, while the latter is 0.95. This theory explains many rock pressure phenomena in solid ground which have not been heretofore understood, such as the compression fracture frequently found on the side wall of a drift. It is pointed out that the state of rock pressure can be inferred to some extent by observing the state of fracture of rock around underground openings.

## 1. Introduction

When an opening is made underground, the stress in the ground is disturbed, causing a stress concentration around the opening. It is known that if the stress at a point reaches a definite limit, fracture of the rock occurs. However, it is not necessarily clear under what conditions the fracture of rock occurs around an opening, though not a few investigations have been published on the theory of rock pressure.

This paper describes the results of investigations of this problem carried out experimentally as well as theoretically. The results are discussed from the practical point of view.

## 2. The theory of the fracture of rock

The conditions for failure of materials differ according to their properties and the stress states to which they are subjected. Thus the general theory of the failure of materials is very complicated. For rock, however, it is believed that the maximum

---

\* Department of Mining Engineering

principal stress theory is applicable to tension fracture, while the internal friction theory or Mohr's theory to compression fracture. That is to say, the tension fracture of rock occurs on a plane where the principal stress reaches the tensile strength of the rock, while the compression fracture of rock occurs on a plane where the shear stress reaches a certain limit which depends upon the normal stress on the plane and the properties of the rock. For a given rock, the relation between the shear stress  $\tau$  and the normal stress  $\sigma$  that causes compression fracture is represented by a curve, called Mohr's limiting curve, on  $\sigma$ - $\tau$  coordinates as shown in Fig. 1. The maximum Mohr's circle representing the state of stress at a point is within the limiting curve as long as no breaking occurs at the point, but it touches the curve when fracture begins. See Circle  $C_1$  or  $C_2$  in Fig. 1. This theory explains the well known fact that rocks behave in different ways when they are in a uniaxial and in a biaxial state of stress<sup>1)</sup>.

Fracture due to tension differs from that due to compression not only in the conditions under which it occurs but also in the mechanism. In the tension fracture of rock, a separation of the two sides along the plane of fracture occurs when cohesion is overcome by tensile stress, while in the compression fracture of rock, the two parts slip along the plane of fracture. Circle  $C_t$  in Fig. 1 represents the Mohr's circle at a point where pure tension fracture occurs.

As one of the principal stresses on the surface of a body is always zero, the condition for compression fracture at the surface of underground openings is rather simple. The maximum Mohr's stress circle " $C_1$ ", in this case, must pass the origin and touch the limiting curve, as shown in Fig. 1. For any given rock, the limiting curve is fixed, and therefore Circle  $C_1$  is also fixed. Consequently the maximum compressive stress represented by point K is definite. It is nothing but the compressive strength of the rock.

On the basis of the above mentioned reasons we can say that tension fracture as well as compression fracture takes place on the surface when the maximum stress (in absolute value) reaches the tensile strength or the compressive strength. It is worth

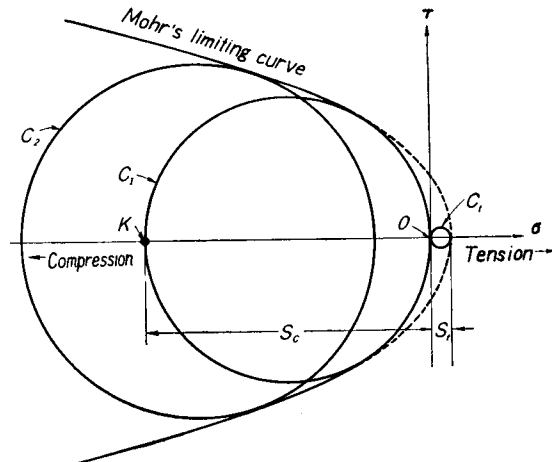


Fig. 1. Mohr's circles and a Mohr's limiting curve for a rock.

noting, however, that the theory of the failure of rock has been established by experiments in which the stresses in test pieces were distributed uniformly. But the actual stress distribution in rock around an opening is not uniform, and there may therefore be room for discussion as to whether or not the theory is applicable in actual cases.

### 3. Model experiment

#### (1) Object and method

Model experiments were carried out in order to obtain data to clarify the conditions under which the fracture of rock occurs around an underground opening. Since it is supposed the properties of the rock have great influence upon rock pressure phenomena, we chose real rocks as the materials for the models. In general, as for the model experiments of phenomena caused by gravity, barodynamics is preferable since it satisfies the law of similarity<sup>2)</sup>. But in our experiments, the use of barodynamics is a disadvantage because the dimensions of the opening are inevitably much smaller than the depth of the opening which makes observation difficult and inaccurate, and also because generation of side pressure is impossible. We decided, therefore, to carry out experiments by compressing models statically. The stress distribution in a model subjected to this experiment is similar to that in a prototype until fracture occurs, as long as the depth from the surface is sufficiently great as compared with the size of the opening<sup>3)</sup>. In this experiment, however, we did not observe or discuss the phenomena after fracture begins.

#### (2) Model

The experiment was carried out with models of horizontal circular levels, as they are easy to produce and offer states of stress well known. The models are rectangular plates of marble or sandstone, 75 mm × 75 mm × 15 mm in size, with circular holes, 10 mm in diameter, at the center of each plate. The marble was taken from Daiyama, Yamaguchi-Prefecture, the sandstone from Tannowa, Osaka-Prefecture. The tensile, compressive and bending strengths of these rocks were carefully tested, using thirty test pieces for each strength test. Table 1 shows the results of these tests.

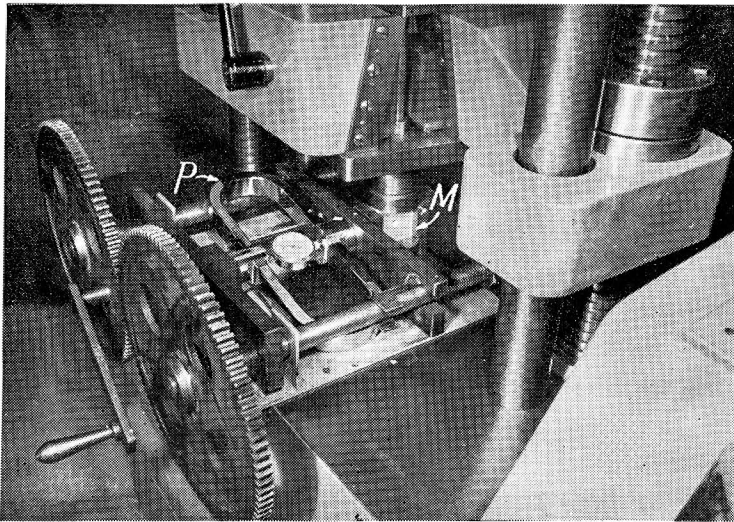
Table 1. Mean strengths of rocks.

Rock	Compressive strength $S_c$ (kg/cm <sup>2</sup> )	Tensile strength $S_t$ (kg/cm <sup>2</sup> )	Bending strength $S_b$ (kg/cm <sup>2</sup> )	$S_c/S_t$	$S_b/S_t$
Marble	896	53	129	16.9	2.4
Sandstone	1577	111	231	14.2	2.1

#### (3) Testing machine

Two kinds of experiments were carried out, uniaxial compression tests and biaxial compression tests. In the former tests, models were compressed vertically and in the

latter in the vertical and horizontal directions simultaneously. The vertical pressure was applied by a 10-ton testing machine, while the horizontal pressure was applied by an apparatus designed and produced by the authors<sup>4)</sup>. It is constructed with two screws, two nuts fed by wheels with gears, a steel ball, a steel plate, a proving ring and so on. The proving ring is for the determination of the horizontal pressure applied. In biaxial compression tests, the horizontal pressure was always kept equal to one fourth of the vertical pressure, by adjusting the feed of the nuts with the handle. In this manner the state of stress in the model was made similar to that in the earth where Poisson's number is 5. Fig. 2 shows a model of marble M being compressed both vertically and horizontally with the apparatus.



M: Model,

P: Proving ring.

Fig. 2. The apparatus to compress the models in vertical and horizontal directions.

#### (4) Results obtained

##### a. Uniaxial compression test

While the load was increased gradually, careful observation was made of the models to ascertain whether any phenomena took place around the circular hole. When the load reached a certain limit, a minute crack appeared due to the tension parallel to the direction of loading just above and below the center of the hole. As the load increased the crack grew, and at last resulted in fracture due to the shear on both sides of the hole. As mentioned earlier, it is beyond the scope of our experiments to study the progress of the fracture.

Now it is difficult to show a model where fracture has just occurred, so that

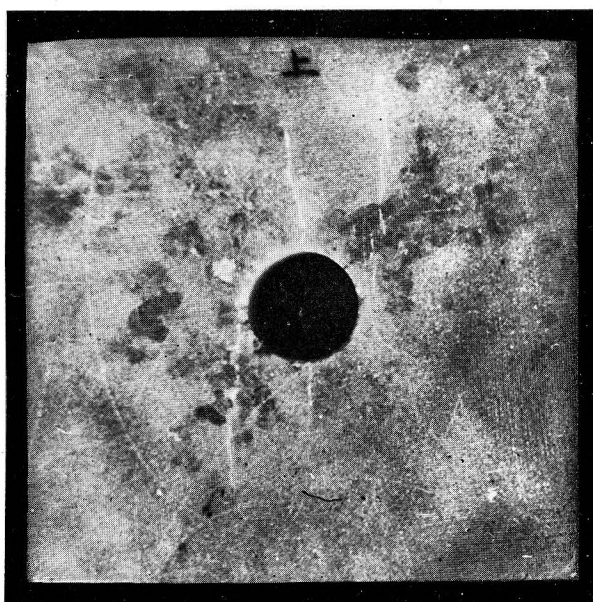


Fig. 3. A model of marble compressed in vertical direction.

we will show in Fig. 3 one of the photographs of the models of marble in which fracture has advanced considerably. The white straight lines running nearly vertically above and below the center of the circular hole in the figure are the tension cracks which grew from the minute cracks that first appeared. The marble shows a whitish pattern on the part where failure has occurred, which makes observation easy. The load under which the failure began was carefully determined for each model. The results are shown in Table 2.

Table 2. Vertical unit load when fracture began to appear.

Kind of tests	Kind of rocks	Number of tests	Vertical unit load (kg/cm <sup>2</sup> ) when fracture begins to appear		
			min.	max.	mean
Uniaxial compression tests	Marble	12	93	160	119
	Sandstone	16	202	325	250
Biaxial compression tests	Marble	15	293	402	352
	Sandstone	15	547	694	610

b. Biaxial compression test

The important facts noticed in biaxial compression tests were that the model did not break unless a far greater load was applied to it than that in a uniaxial compression test, and that when at last fracture appeared it was not tension fracture but compression fracture on the side wall of the circular hole.

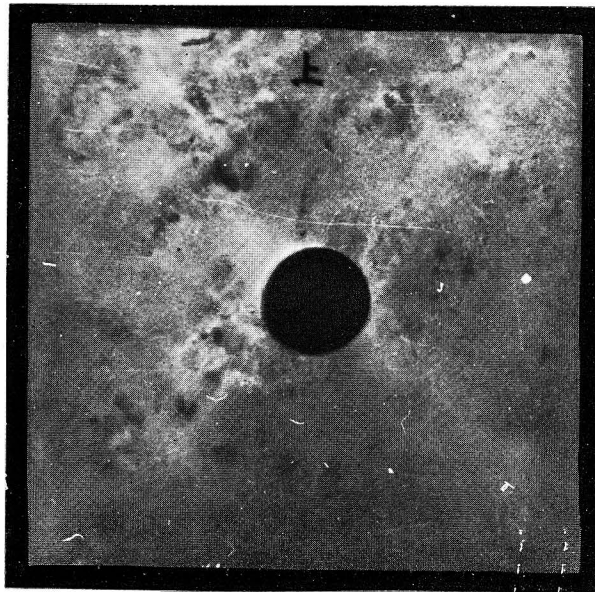


Fig. 4. A model of marble compressed in vertical and horizontal directions simultaneously.

Fig. 4 shows one of models of marble in which failure has progressed considerably in a biaxial compression test. The X-shaped whitish pattern that can be seen around the hole was caused by slips in the marble. Comparing Fig. 4 with Fig. 3, we can see that there is a great difference in the state of fracture between the uniaxial and the biaxial compression tests. The vertical unit load under which the failure begins in each model was carefully observed. The results are also shown in Table 2.

(5) Theoretical considerations on the conditions for fracture

It is supposed that the fracture on the surface of rock would occur, as described before, when the maximum principal stress (in absolute value) reaches the tensile or the compressive strength of the rock or else some other limit which depends upon those strengths. The true stress in a model, however, can not be estimated because rock has a non-linear elasticity as well as some plasticity, and all we can do is to find the theoretical stress, assuming that the model is a perfect elastic body.

Consider an infinite elastic plate with a circular hole. Taking polar coordinates  $(r, \theta)$ , the origin being at the center of the hole, as shown in Fig. 5,

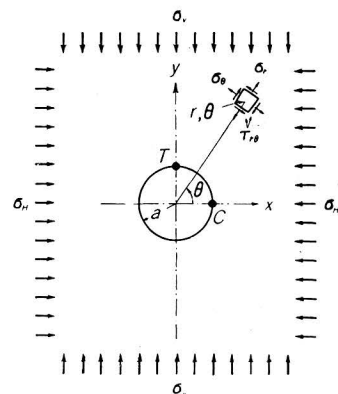


Fig. 5.

the normal stresses  $\sigma_r$  and  $\sigma_\theta$  and the shear stress  $\tau_{r\theta}$  at a point  $(r, \theta)$  are represented by following equations according to the theory of elasticity<sup>5)</sup>.

$$\left. \begin{aligned} \sigma_r &= \frac{\sigma_V}{2} \left\{ 1 - \frac{a^2}{r^2} - \left( 1 - 4 \frac{a^2}{r^2} + 3 \frac{a^4}{r^4} \right) \cos 2\theta \right\} + \frac{\sigma_H}{2} \left\{ 1 - \frac{a^2}{r^2} + \left( 1 - 4 \frac{a^2}{r^2} + 3 \frac{a^4}{r^4} \right) \cos 2\theta \right\}, \\ \sigma_\theta &= \frac{\sigma_V}{2} \left\{ 1 + \frac{a^2}{r^2} + \left( 1 + 3 \frac{a^4}{r^4} \right) \cos 2\theta \right\} + \frac{\sigma_H}{2} \left\{ 1 + \frac{a^2}{r^2} - \left( 1 + 3 \frac{a^4}{r^4} \right) \cos 2\theta \right\}, \\ \tau_{r\theta} &= \frac{\sigma_V}{2} \left\{ 1 + 2 \frac{a^2}{r^2} - 3 \frac{a^4}{r^4} \right\} \sin 2\theta - \frac{\sigma_H}{2} \left\{ 1 + 2 \frac{a^2}{r^2} - 3 \frac{a^4}{r^4} \right\} \sin 2\theta, \end{aligned} \right\} \quad (1)$$

where  $a$  is the radius of the hole,  $\sigma_V$  and  $\sigma_H$  are the vertical and horizontal stresses respectively at some sufficient distance away from the hole. At the surface of the hole,  $r$  is equal to  $a$ , so that we get from eq. (1)

$$\left. \begin{aligned} \sigma_r &= 0, \\ \sigma_\theta &= \sigma_V(1 + 2 \cos 2\theta) + \sigma_H(1 - 2 \cos 2\theta). \end{aligned} \right\} \quad (2)$$

Fig. 6 shows the distribution of  $\sigma_\theta$  on the surface of the hole under the following boundary conditions:

- (i)  $\sigma_V = p_0, \sigma_H = 0$  (thick line),
- (ii)  $\sigma_V = p_0, \sigma_H = p_0/4$  (dotted line),
- (iii)  $\sigma_V = 0, \sigma_H = p_0$  (chain line).

These curves are drawn by plotting  $\sigma_\theta/p_0$  at any point on the normal from the point to the surface. Compressive stress is plotted outside the surface and tensile stress inside it. As the state of stress is symmetrical with respect to the axes of geometrical symmetry, each curve is drawn on one side of the axis.

Let the intersecting points of the horizontal and vertical axes with the surface of the circular hole be C and T respectively, and let the tangential stress at points C and T be denoted simply by  $\sigma_C$  and  $\sigma_T$ , then they can be obtained by putting  $\theta=0$  and  $\theta=\pi/2$  respectively in eq. (2).

Now let us use the same letters C and T to denote the corresponding points on the model, and let the theoretical tangential stresses at points C and T, under the assumption that the model is perfectly elastic, be  $\sigma_C'$  and  $\sigma_T'$ . Here the sign (') is added to show that these stresses are under the assumption of perfect elasticity. From eq. (2)  $\sigma_C'$  and  $\sigma_T'$  are at once obtained by putting  $\sigma_V=p_0$  and  $\sigma_H=0$  for the uniaxial compression tests and by putting  $\sigma_V=p_0$  and  $\sigma_H=p_0/4$  for the biaxial compression tests. Thus we get for the uniaxial compression tests

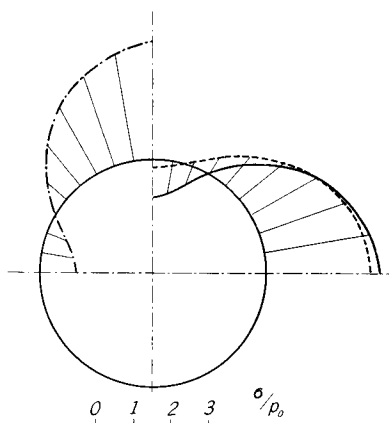


Fig. 6. Distribution of the tangential stress along the circular hole under various boundary conditions.

$$\left. \begin{aligned} \sigma_{\sigma'} &= 3p_0, \\ \sigma_{\tau'} &= -p_0, \end{aligned} \right\} \quad (3)$$

and for the biaxial compression tests

$$\left. \begin{aligned} \sigma_{\sigma'} &= 2.75p_0, \\ \sigma_{\tau'} &= -0.25p_0. \end{aligned} \right\} \quad (4)$$

In applied mechanics, tensile stress is assumed positive, compressive stress negative. Consequently  $p_0$  and  $\sigma_{\sigma'}$  are negative, while  $\sigma_{\tau'}$  is positive. The theoretical stresses  $\sigma_{\sigma'}$  and  $\sigma_{\tau'}$  that appear when fracture begins to occur in the model can be obtained from eq. (3) and (4) by substituting  $p_0$  with the mean unit loads shown in Table 2. The results are tabulated in Table 3.

Table 3. Theoretical stress at the beginning of failure.

Kind of tests	Kind of rocks	Number of tests	Failure begins to appear		Theoretical stresses (kg/cm <sup>2</sup> )		Remarks
			at	under a mean vertical unit load of	$-\sigma_{\sigma'}$	$\sigma_{\tau'}$	
Uniaxial compression test	Marble	12	Point T	119 kg/cm <sup>2</sup>	357	119	For marble $S_c=896$ kg/cm <sup>2</sup> $S_t= 53$ kg/cm <sup>2</sup>
	Sandstone	16	Point T	250 kg/cm <sup>2</sup>	750	250	
Biaxial compression test	Marble	15	Point C	352 kg/cm <sup>2</sup>	968	83	For sandstone $S_c=1577$ kg/cm <sup>2</sup> $S_t= 111$ kg/cm <sup>2</sup>
	Sandstone	15	Point C	610 kg/cm <sup>2</sup>	1678	153	

It is worth noting in this table that the tension crack does not appear until the theoretical maximum tensile stress  $\sigma_{\tau'}$  reaches a magnitude about two times the tensile strength  $S_t$  in the uniaxial compression tests, and that in the biaxial compression tests the compression fracture occurs already when the theoretical maximum compressive stress  $-\sigma_{\sigma'}$  becomes but a little higher than the compressive strength  $S_c$ , while at point T there appears no tension crack at the moment of the beginning of compression fracture even though  $\sigma_{\tau'}$  exceeds  $S_t$  considerably. From these facts we can understand how different the circumstances are between tension and compression fractures around the hole.

The ratio of tensile or compressive strength to the theoretical maximum tensile or compressive stress respectively at the instant of fracture is as follows:

For tension fracture on the models of marble and sandstone  $S_t/\sigma_{\tau'}=0.45$ ,  
 for compression fracture on the models of marble  $S_c/-\sigma_{\sigma'}=0.93$ ,  
 and for compression fracture on the models of sandstone  $S_c/-\sigma_{\sigma'}=0.94$ .

On the basis of these experimental results, the authors made the following assumption in regard to the conditions for fracture around an underground opening.

“Let the theoretical maximum tensile and compressive stress under the assumption that the ground is perfectly elastic be denoted by  $\sigma_{\tau'}$  and  $\sigma_{\sigma'}$ , then tension or compression fracture will appear when  $k_T\sigma_{\tau'}$  or  $-k_C\sigma_{\sigma'}$  reaches the tensile or



compressive strength of the rock, where the factors  $k_T$  and  $k_C$  are estimated to be approximately 0.45 and 0.95 respectively from our experiments."

Of course it is supposed that the factors are dependent on the accuracy of the determination of  $S_t$  and  $S_c$ , and that they will probably depend upon the nature of the rock. The assumption with regard to the condition of fracture does not contradict the fact that in the biaxial compression test no tension fracture occurs at point T at the moment when there appears a compression fracture at point C, because  $k_T\sigma_T'$  is smaller than  $S_t$  in both marble and sandstone models, though  $\sigma_T'$  itself is far greater than  $S_t$ .

Now let us discuss briefly certain aspects of the assumption. The theoretical stresses  $\sigma_T'$  and  $\sigma_C'$  would be true if the rock had perfect elasticity, i.e. if the rock obeyed closely Hooke's law and moreover if Young's modulus were constant through all the tension and compression ranges. According to the theory of elasticity tensile stress appears only in very limited areas above and below the circular hole, while all the remaining parts are subjected to more or less compressive stress. It is easily imagined that the actual stress in the area where compression fracture will occur may be somewhat smaller than the theoretical value because the stress-strain diagram of rock is not straight but curved and Young's modulus decreases a little with an increase in stress, especially at higher stresses. Under these circumstances, we can understand that compression fracture would occur when  $-k_C\sigma_C'$  reaches the compressive strength of rock,  $k_C$  being a factor slightly smaller than unity, say 0.95. It is difficult, however, to understand in this way the fact that tension fracture occurs when  $k_T\sigma_T'$  reaches the tensile strength of rock,  $k_T$  being a factor, in this case, far smaller than unity, say 0.45, since the stress strain diagram of rock is not curved so much as to make it necessary to introduce such a great correction.

The distribution of the theoretical normal stress on the vertical section TT' through the center is as shown in Fig. 7. One of the normal stress  $\sigma_\theta$  is maximum at point T and decreases with the distance from the point. After becoming zero, it turns into a negative stress, i.e. compressive stress. When tension fracture begins to appear at point T, the stress on the Section TT' will distribute itself over the whole range of the tensile stress-strain curve as well as on a small range at the foot of the compressive stress-strain curve of the rock. Consequently, on the Section TT' the average Young's modulus of the rock within the range of tensile stress differs from that outside it. Considering these circumstances it may not always be difficult to accept that there is a great difference between the theoretical stress at point T and the tensile strength at the moment tension fracture begins.

The state of affairs in the bending fracture of rock is much like the tension fracture at the surface of the hole in the models. If a beam is perfectly elastic, the

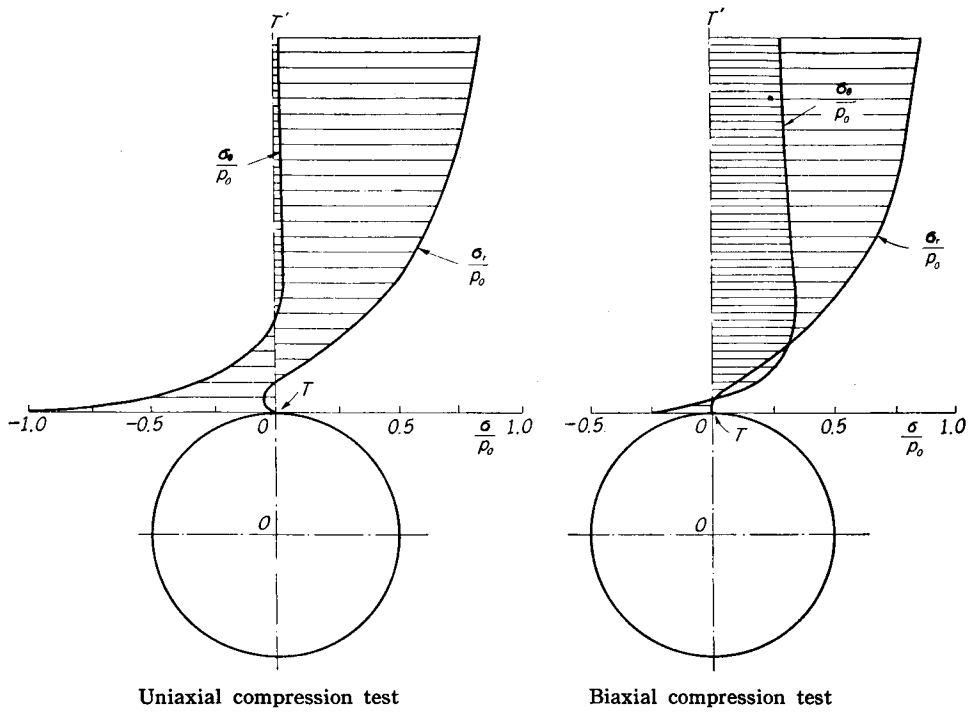


Fig. 7. Stress distribution on the vertical section through the center of the circular hole.

distribution of stress on the section along which fracture is to occur would be linear as illustrated by a dotted straight line I in Fig. 8.

But since the stress-strain curve of rock is curved and the tensile strength is far lower than the compressive strength, the actual stress distribution may be something like Curve II

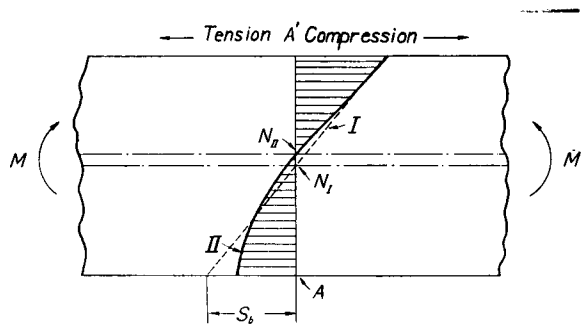


Fig. 8. Stress distribution on a cross-section of a beam under bending moment.

in Fig. 8, the neutral axis shifting a little to the compression side, namely from  $N_I$  to  $N_{II}$ . From this figure we can see that at the moment of fracture the actual maximum tensile stress is remarkably smaller than the theoretical maximum tensile stress, called the bending strength or the bending modulus of rupture. If it is assumed that the actual maximum tensile stress at the moment when fracture begins is equal to the tensile strength, we can say that the bending strength  $S_b$  is much greater than the tensile strength  $S_t$ . For marble and sandstone employed in our model experiments,

the ratio  $S_t/S_b$  are 0.41 and 0.48 respectively. It is noticed that they are approximately equal to the ratio  $S_t/\sigma_T'$  in the uniaxial compression tests. These two kinds of phenomena concerning fracture of rock, i.e. the bending fracture of a beam and the tension fracture around a hole, therefore, have not only a similar cause but also an approximately equal ratio of the tensile strength to the theoretical maximum tensile stress.

The authors have attempted to examine experimentally whether or not we can consider that the actual maximum tensile stress at the moment fracture begins is equal to the tensile strength, but no conclusion has yet been reached. Nevertheless, from the theoretical point of view it seems that the assumption, described before, in regard to the condition of fracture around an opening is not unreasonable.

#### 4. Field observations accompanied by photo-elastic experiments

##### (1) Purpose

It has been generally accepted that the fracture of rock, if it happens, will usually take place at the roof of an opening, because according to the theory of elasticity, there occurs, on the roof, considerable tensile stress that may exceed the tensile strength of rock, though the high compressive stress on the side walls does not exceed the compressive strength<sup>6)</sup>.

According to the authors' assumption, however, fracture of rock takes place under the following circumstances. Let  $\sigma_C'$  and  $\sigma_T'$  be the theoretical maximum compressive and tensile stress around an opening with the assumption that the ground is perfectly elastic.  $\sigma_C'$  and  $\sigma_T'$  depend on the topography, the shape of the opening and the boundary conditions. Now if the conditions are such that

$$\frac{-k_C\sigma_C'}{k_T\sigma_T'} < \frac{S_c}{S_t}$$

and  $k_T\sigma_T'$  reaches  $S_t$ , then tension fracture will first occur at the point of the maximum tensile stress. On the other hand if the conditions are such that

$$\frac{-k_C\sigma_C'}{k_T\sigma_T'} > \frac{S_c}{S_t}$$

and  $-k_C\sigma_C'$  reaches  $S_C$ , then compression fracture will first take place at the point of the maximum compressive stress. The strength ratio  $S_C/S_T$  is about 15 or more for most rocks in the authors' tests.

Now we must investigate whether the authors' assumption described above is really applicable to the fracture of rock around an underground opening. This investigation should depend upon field experiments, and if possible in homogeneous and isotropic ground. Field experiments under various boundary conditions, however, are

difficult to carry out, so that the authors have investigated this problem by observing on what part of the surface of horizontal levels fracture takes place.

In this discussion accurate knowledge is necessary about the states of stress around several kinds of openings under the assumption that the ground is perfectly elastic. Photo-elastic experiments were carried out for this purpose.

(2) Stress analysis by photo-elasticity

Assuming that the surface of ground is horizontal and that the rock pressure is caused by the weight of the ground, namely that it is not necessary to consider the influence of diastrophism, the vertical and horizontal stress  $\sigma_V$  and  $\sigma_H$  before an opening is produced in a homogeneous and isotropic elastic ground are given as :

$$\left. \begin{aligned} \sigma_V &= \gamma h, \\ \sigma_H &= \gamma h/m - 1, \end{aligned} \right\} \quad (5)$$

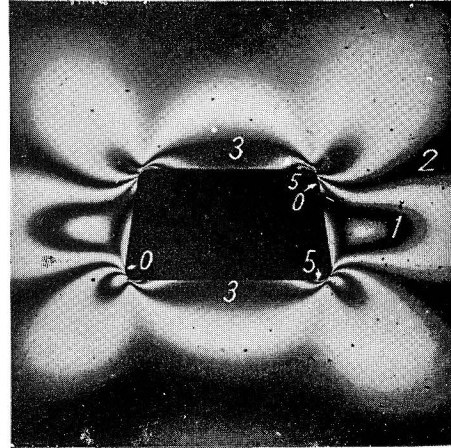
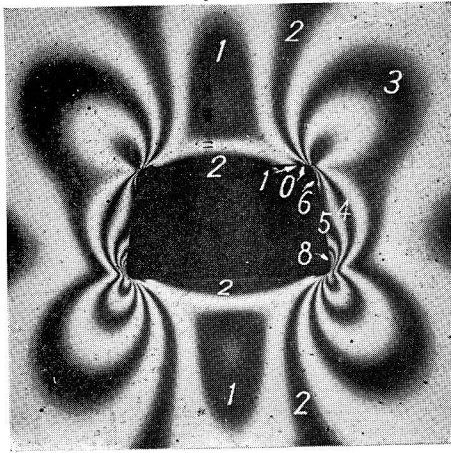
where  $\gamma$  and  $m$  are the specific weight and the Poisson's number of the ground respectively and  $h$  the depth of the opening. The state of stress after a level is driven in such ground can be obtained analytically if the cross-section of the level is a circle or an ellipse or some other geometrical figure, but if the cross-section is of some other shape we can not but resort to photo-elastic experiments.

In discussing the conditions for fracture of rock, it is necessary to refer to the theoretical maximum stresses as accurately as possible. In particular we must pay attention to the influence of the horizontal pressure that existed before a level was driven, since the horizontal pressure greatly affects the tensile stress on the surface of a level. Several investigations by means of photoelastic experiments have been hitherto published on the states of stress around levels of various shapes<sup>7)</sup>. It seems, however, that there still remains some room for study of this problem, especially regarding the influence of the horizontal pressure, so that the authors decided to carry out two dimensional photoelastic experiments again to obtain the stress on the surface of various shapes of levels under several boundary conditions.

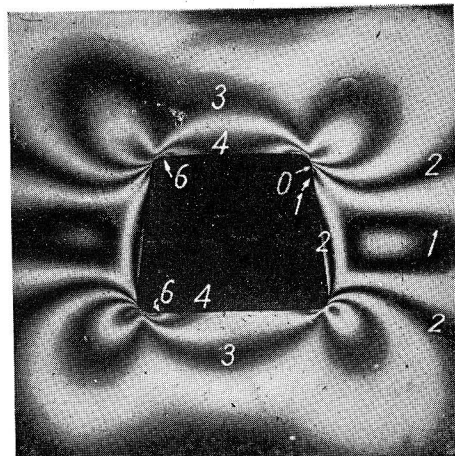
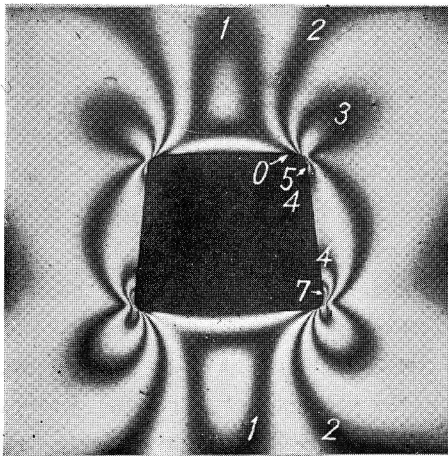
The models were rectangular plates 150 mm  $\times$  150 mm  $\times$  10 mm made of ethoxylin resin having holes of various shapes at the center, one to each model. First these models were compressed uniformly in the vertical direction and stress patterns were observed. Then they were compressed again in the horizontal direction and observed. Fig. 9 shows the stress patterns obtained, the numerals on the stress fringes being their fringe orders. The model fringe value noted on the right of each pair of figures multiplied by any fringe order gives the principal stress difference  $\sigma_1 - \sigma_2$  at any point on the fringe. From these figures, the distribution of tangential stress on the inner surface of each hole is easily determined. Fig. 10 shows the curves illustrating these distributions on the surface of several shapes of holes, drawn in the same manner as

Vertical compression

Horizontal compression



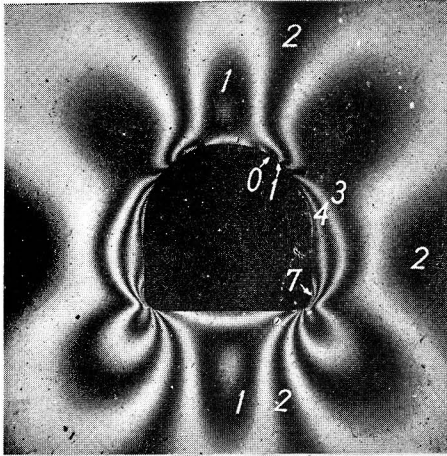
Height of the hole  $h=20$  mm, unit load  $p_0=24.1$  kg/cm<sup>2</sup>,  
model fringe value=0.60  $p_0=14.5$  kg/cm<sup>2</sup>.



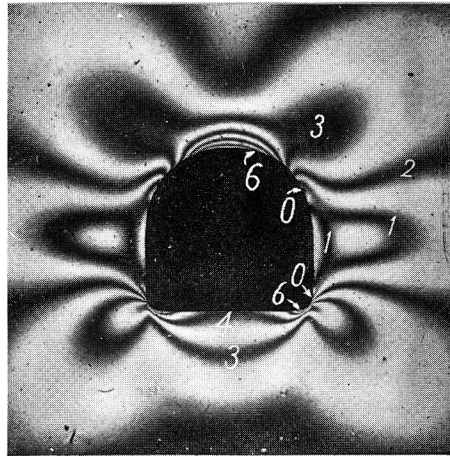
Height of the hole  $h=30$  mm, unit load  $p_0=26.0$  kg/cm<sup>2</sup>,  
model fringe value=0.60  $p_0=15.6$  kg/cm<sup>2</sup>.

Fig. 9. Stress patterns of plates with several shapes of openings subjected to vertical and horizontal compression separately.

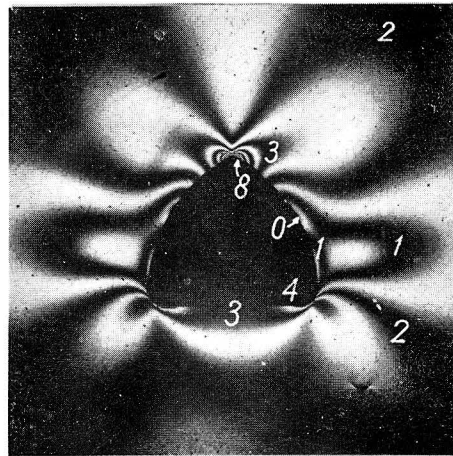
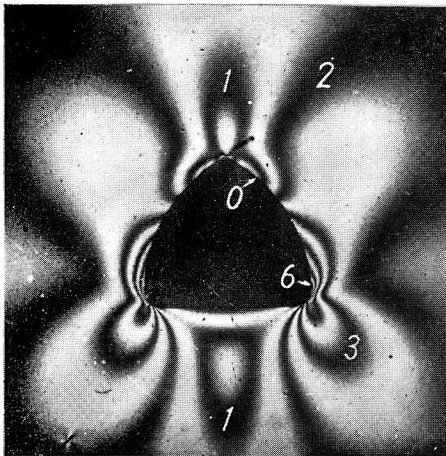
Vertical compression



Horizontal compression



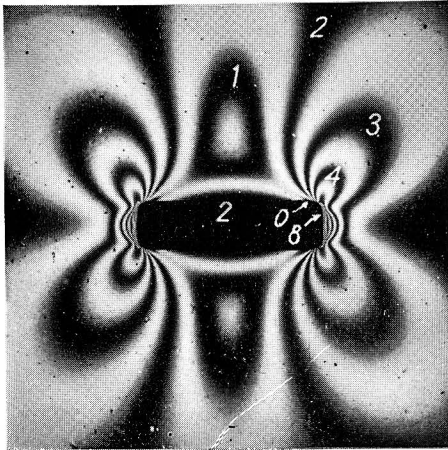
Height of the hole  $h=30$  mm, unit load  $p_0=26.0$  kg/cm<sup>2</sup>,  
model fringe value= $0.60$   $p_0=15.6$  kg/cm<sup>2</sup>.



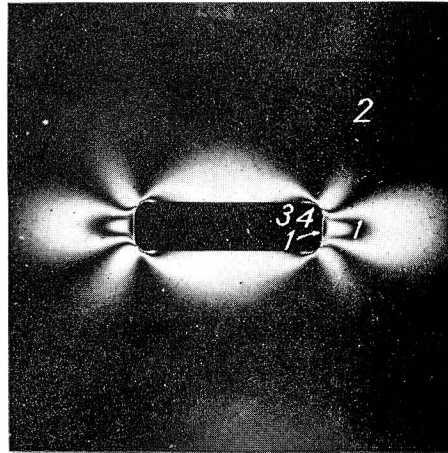
Height of the hole  $h=26$  mm, unit load  $p_0=25.4$  kg/cm<sup>2</sup>,  
model fringe value= $0.64$   $p_0=16.4$  kg/cm<sup>2</sup>.

Fig. 9. (Continued from the preceding page).

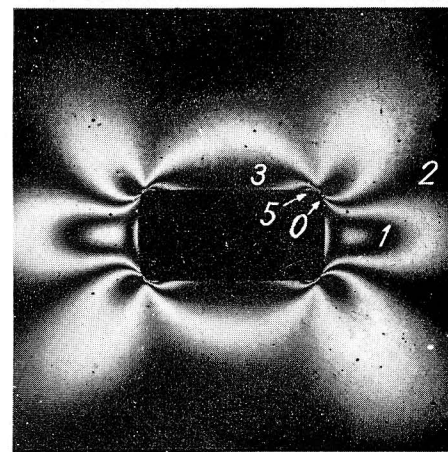
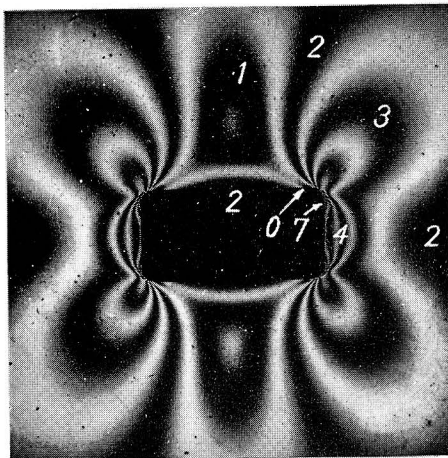
Vertical compression



Horizontal compression

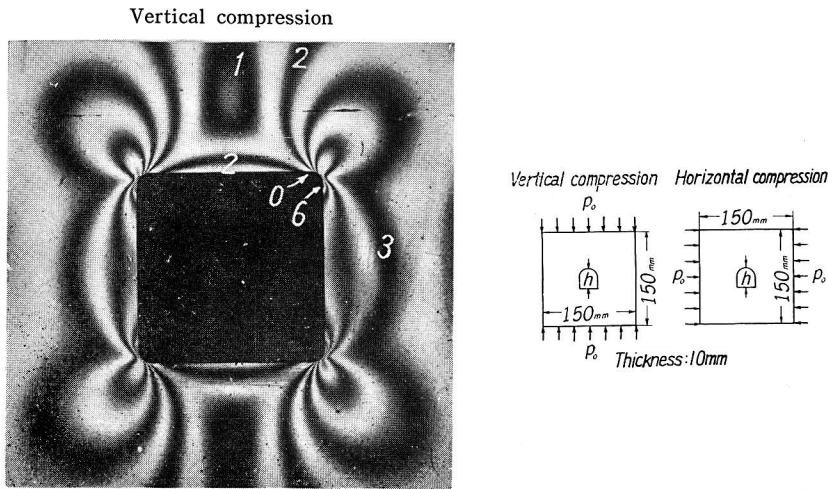


Height of the hole  $h=8$  mm, unit load  $p_0=24.1$  kg/cm<sup>2</sup>,  
model fringe value=0.60  $p_0=14.5$  kg/cm<sup>2</sup>.



Height of the hole  $h=26$  mm, unit load  $p_0=24.1$  kg/cm<sup>2</sup>,  
model fringe value=0.60  $p_0=14.5$  kg/cm<sup>2</sup>.

Fig. 9. (Continued from the preceding page.)



Height of the hole  $h=37$  mm, unit load  $p_0=26.0$  kg/cm<sup>2</sup>, model fringe value= $0.53 p_0=13.8$  kg/cm<sup>2</sup>.

Fig. 9. (Continued from the preceding page.)

in Fig. 6. Thick lines, dotted lines and chain lines in the figure represent the stress distributions under three different boundary conditions as follows:

- (i)  $\sigma_V = p_0, \sigma_H = 0$  (thick lines),
- (ii)  $\sigma_V = p_0, \sigma_H = p_0/4$  (dotted lines),
- (iii)  $\sigma_V = 0, \sigma_H = p_0$  (chain lines).

Stress distributions under any other boundary conditions can be obtained from the stress distributions under the two boundary conditions (i) and (iii) by simple calculation applying the law of superposition. It is supposed, that in ordinary ground the boundary conditions would be approximately (ii) or thereabouts.

The stress curves in Fig. 10 point out that the addition of the horizontal loading, though small, makes the tensile stress appearing on the roof or floor decrease remarkably while the compressive stresses on the side walls suffer but little reduction, and even a slight increase near the corners. The theoretical maximum compressive and tensile stresses  $\sigma_C'$  and  $\sigma_T'$  can be evaluated for each model from Fig. 10. The relation between the ratio  $-\sigma_C'/\sigma_T'$  as well as  $-k_C\sigma_C'/k_T\sigma_T'$  and the boundary conditions are shown in Fig. 11 for various shapes of levels. Point C and T on this figure indicate the points of the maximum compressive and tensile stresses respectively. In some shapes of levels point C shifts with variations in the boundary conditions, though slightly, but in Fig. 11 only the point referring to the condition  $\sigma_H/\sigma_V=0.25$  is shown. The boundary condition,  $\sigma_H/\sigma_V=0$ , is for the special ground in which there is no horizontal pressure before a level is driven. The boundary condition of ordinary ground may well be such that  $\sigma_H/\sigma_V$  is between 0.25 and 0.4, owing to the following reason.



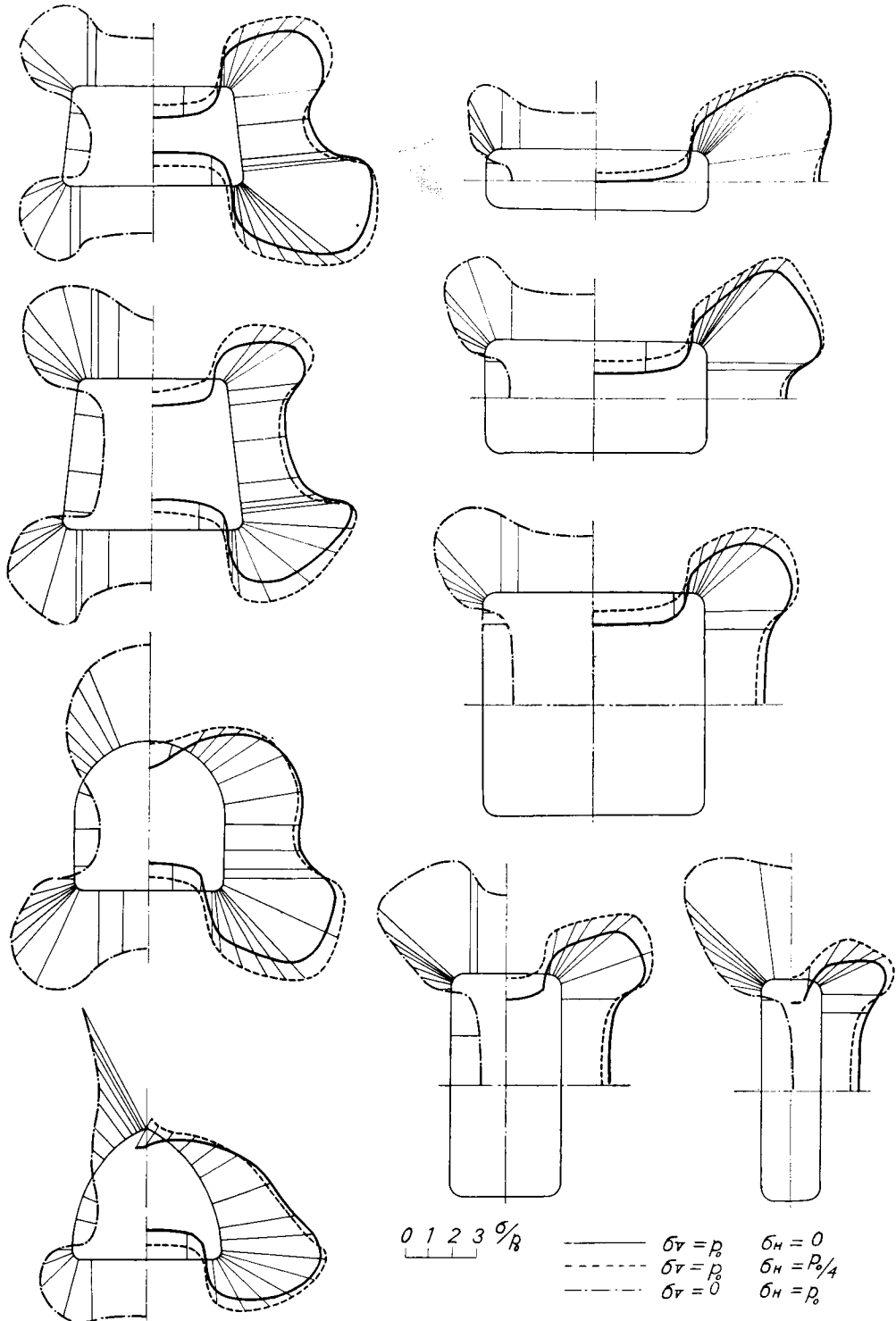


Fig. 10. Distribution of the tangential stress on the inner surface of the hole.

The initial horizontal pressure  $\sigma_H$  is dependent upon the Poisson's number of ground, which is inherent in each rock and dependent upon the stress the rock is subjected to. From our experiments it is supposed that under comparatively high pressure, the Poisson's number of most rocks may be between 5 and 3.5. Consequently  $\sigma_H/\sigma_V$  is assumed to be between 0.25 and 0.4.

(3) Discussion of the assumption concerning fracture of rock by field observation.

If we can discuss the fracture of rock around an underground opening by comparing the theoretical maximum stress with the strength of rock either directly or by introducing a slight modifica-

tion, it is expected, referring to Fig. 11, that tension fracture will take place first, if any, on the roof or floor, in ordinary levels under two directional rock pressure, because  $-\sigma_C'/\sigma_T'$  is generally less than  $S_c/S_t$ , namely about 15. But if the authors' assumption is accepted, i.e. if fracture of rock occurs when  $-k_C\sigma_C'$  or  $k_T\sigma_T'$  reaches  $S_c$  or  $S_t$  respectively, it is expected, referring to Fig. 11, that under two directional rock pressure the compression fracture on the side walls will begin earlier than tension fracture on the roof in ordinary levels; but that under one directional rock pressure, however, the tension fracture will take place first. The opinion that the roof or floor is the weakest part of the surface of an opening has been widely accepted, but it does not agree with the conclusion derived from the authors' assumption.

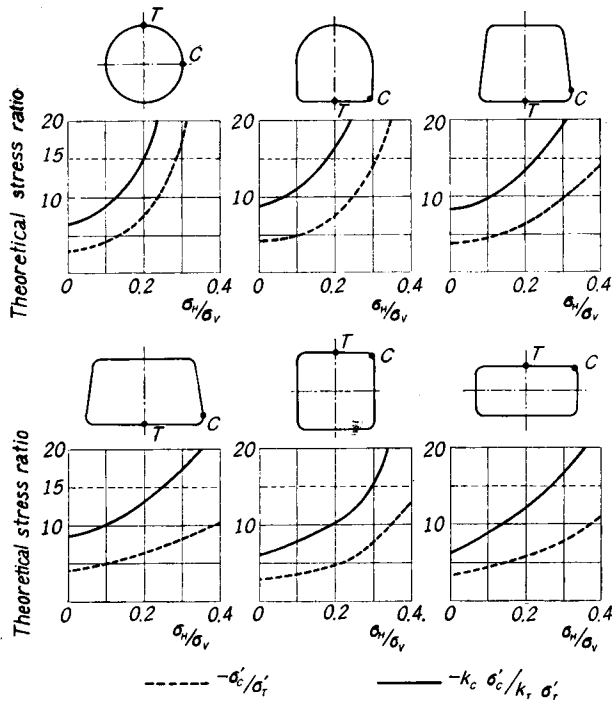
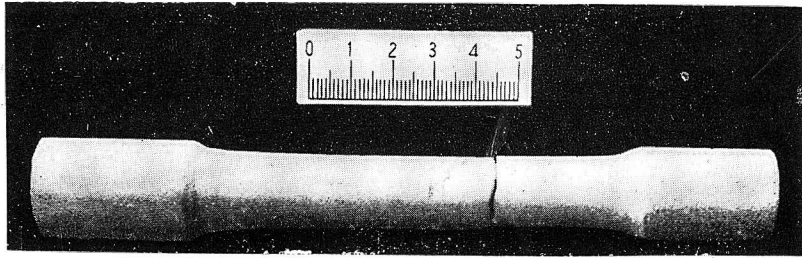


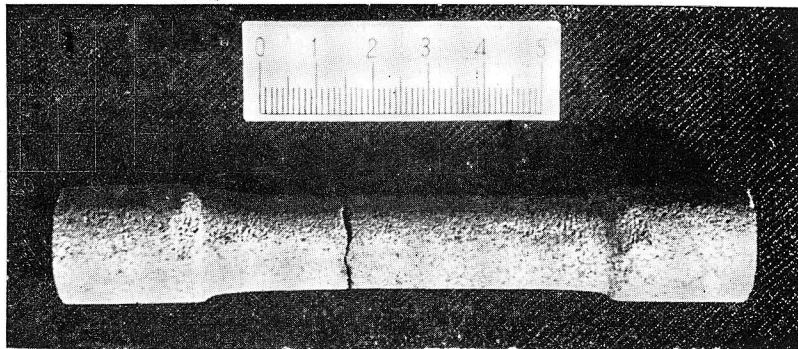
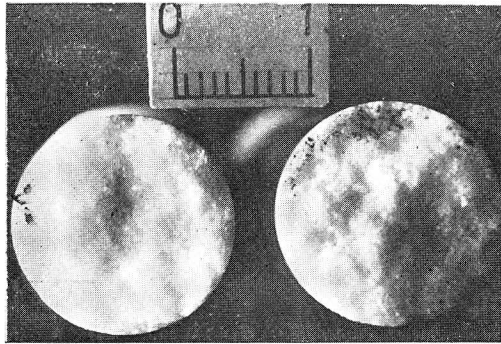
Fig. 11. The theoretical stress ratios  $-\frac{\sigma_C'}{\sigma_T'}$  and  $-\frac{k_C\sigma_C'}{k_T\sigma_T'}$  for various shapes of levels.

Observations were made underground to see which idea is correct. The position and the appearance of fracture were carefully observed in levels, considering the probable theoretical maximum stresses,  $\sigma_C'$  and  $\sigma_T'$ . The appearance of fracture affords the material for distinguishing between tension and compression fracture. From tension and compression tests of rocks we can see that tension fracture appears

generally on a plane normal to the external force, while compression fracture takes place on a large number of planes, either making acute angles with or being nearly parallel to the direction of the external force, as shown in Fig. 12 and 13.



Marble



Sandstone

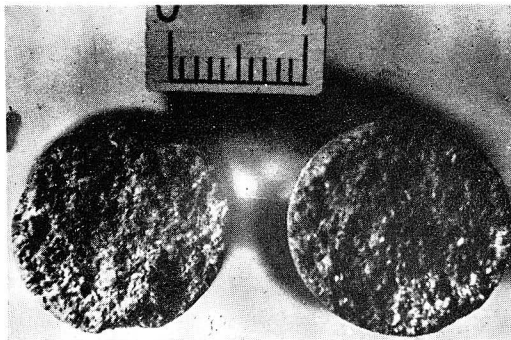
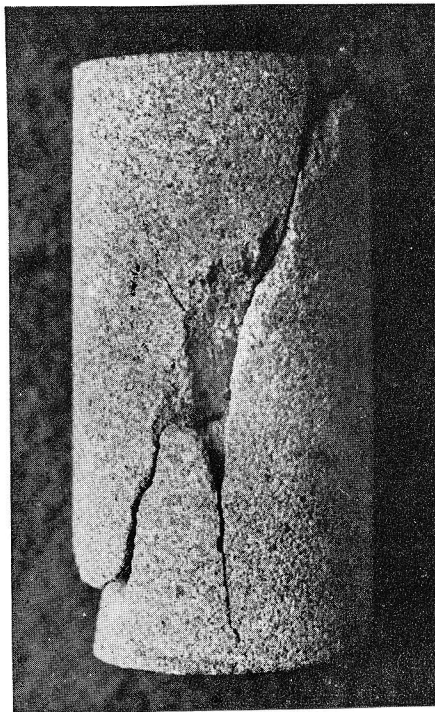


Fig. 12. Fracture of rocks by tension tests.



Marble



Sandstone

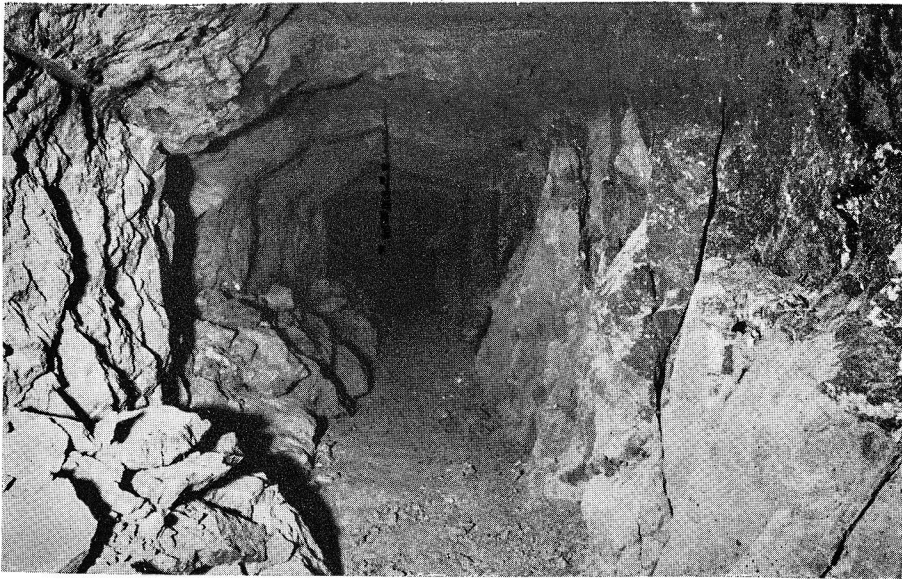


Granite

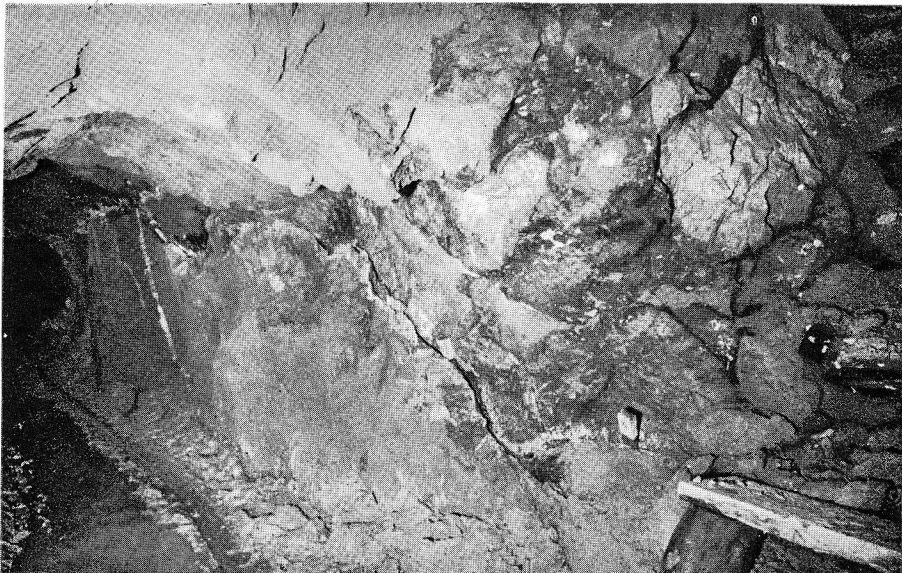
Fig. 13. Fracture of rocks by compression tests.

Several manners of fracture to be seen underground will be shown below. In levels driven in a ground subjected to high pressure, we can frequently see compression fracture on the side wall but no tension fracture on the roof as shown in Fig. 14. Such a phenomenon is more remarkable at a junction of two levels as shown in Fig. 15. In such ground as there is no horizontal pressure, the state of affairs is quite different. Such an example is a level driven in a vertical pillar supporting a heavy load. Tension cracks appear on the roof and the floor while compression fracture is hardly to be seen on the side wall as shown in Fig. 16.

From this field observation it was found that compression fracture takes place



(Kamioka Mine)



(Kamioka Mine)

Fig. 14. Compression fracture on the side walls of levels.



(Matsuo Mine)

Fig. 15. Compression fracture at the junction of levels.

first in ordinary levels driven in ground under two directional pressure, but that when the ground stands under one directional pressure, tension fracture appears first. These results lead us to the conclusion that the authors' assumption on the fracture of rock around mine openings is valid. Therefore we can foresee the possible fracture around mine openings to some extent by this assumption, taking into account the topography, underground conditions and the strength of rock.

##### **5. Observation of fracture of rock as an aid to infer the state of rock pressure.**

When the ground is homogeneous and isotropic, the rock pressure phenomena would be predicted theoretically in the way described above. But as these conditions are rarely satisfied in practice, and moreover as there are frequently fissures in the ground, accurate prediction will be impossible. It has been proved, however, from this investigation, that observation of fracture of rock around mine openings is helpful in investigating the state of rock pressure in the ground. In the first place the appearance of fracture enables us to know whether it is due to tension or compression. Presence of fracture of rock at a certain point shows that stress at the point reached the strength of the rock at one time and that the stress in the neighbourhood of the point is at present near that strength. When we find fractures on the walls of underground openings, there will still be time before the ground caves, because the stress in the ground is always greater at the wall than in the interior. From the fundamental knowledge about the theoretical stress around mine openings, the presence



(Kamioka Mine)



(Kamioka Mine)

Fig. 16. Tension fracture on the roof and the floor.



(Yanahara Mine)



(Yanahara Mine)

Fig. 17. Tension fracture on the side wall.





(Kamioka Mine)

Fig. 17. (Continued from the preceding page.)

of fracture of rock as well as the strength of rock, it will be possible to infer the present state of rock pressure in the ground to some extent.

We have already discussed the compression fracture on the wall or the tension fracture on the roof of a level, therefore some other rock pressure phenomena will be outlined below. Vertical pillars are frequently subjected to bending, rather than pure compression, and break by buckling. On one side of such pillars we can see tension fracture and on the other side compression fracture. If the ground is subjected to tension in a vertical direction, tension, crack will appear on the side wall of the level driven into it. Fig. 17 shows such levels driven into the ground above a large goaf. The ground might have been under tension probably due to the self weight of the rock around the level.

## 6. Conclusion

The conditions under which fracture of rock occurs around an underground opening were investigated by model experiments, photoelastic experiments and field observations accompanied by analysis. It was found from this investigation that fracture of rock takes place when the theoretical maximum stress, tensile or compressive, under the assumption that the ground is perfectly elastic, multiplied by a corresponding factor reaches the tensile or compressive strength of the rock. There is a great difference between the factor for tension fracture and that for compression fracture, namely that the former is about 0.45 while the latter is 0.95. Many rock pressure phenomena in elastic ground have been explained well with this theory. For example, the compres-

sion fracture frequently found on the side wall of a level in heavy ground can be understood by this theory, owing to the influence of the horizontal rock pressure and the correction to be applied for the theoretical tensile stress. Such a phenomenon is hard to explain by merely depending upon the theory of elasticity. It was also pointed out that the state of stress in the ground can be inferred to some extent by observing the fracture of rock around an underground opening.

#### **Acknowledgement**

A part of the expense of this study was defrayed by the Scientific Research Grant from the Ministry of Education to which the authors wish to express their hearty gratitude.

#### **References**

- 1) V. Kármán; *Z. V. D. I.*, **55**, 1754, (1911).
- 2) P. B. Bucky; *A. I. M. E. Tech. Pub.*, No. 425, (1931).  
Louis A. Panek; U. S. Bureau of Mines, Report of Investigation 4883, (1952).  
E. Mikumo, Y. Hiramatsu, Y. Fujinaka; *J. Mining Inst. of Japan*, **68**, 307-311, (1952).
- 3, 4) Y. Hiramatsu, Y. Oka; *J. Mining Inst. of Japan*, **72**, 439-444, (1956).
- 5) G. Kirsch; *Z. V. D. I.*, **42**, 797, (1898).
- 9) Kommerell; *Statische Berechnung von Tunnelmauerwerk*, S. 69, (1912).  
Fenner; *Glückauf*, **74** Jahrg., 681-695, (1938).
- 7) G. Dorstewitz; *Archiv für Bergbauliche Forschung*, **1**, (1940).  
W. I. Duvall; U. S. Bureau of Mines, Report of Invest. No. 4192, (1948).  
Kaneshige, Okamura, Kawamoto; *J. of Mining Inst. of Kyushu*, **25**, 307-316, (1957).